ISSN 1674-1056
http://cpb.iphy.ac.cn
http://iopscience.iop.org/cpb
中国物理 B
Chinese Physics
中国物理 Chinese Physics B

Isomerism and coordination mode effects on two-photon absorption of tris(picolyl)amine-based fluorescent probes for zinc ions

Ke Zhao(赵珂), Jun Song(宋军), Mei-Yu Zhu(朱美玉), Han Zhang(张瀚), Chuan-Kui Wang(王传奎)
Citation: Chin. Phys. B . 2018, 27(10): 103301. **doi:** 10.1088/1674-1056/27/10/103301

Journal homepage: http://cpb.iphy.ac.cn; http://iopscience.iop.org/cpb

What follows is a list of articles you may be interested in

High-power ultraviolet 278-nm laser from fourth-harmonic generation of an Nd: YAG amplifier in CsB_3O_5 crystal

Miao He(何苗), Feng Yang(杨峰), Cheng Dong(董程), Zhi-Chao Wang(王志超), Lei Yuan(袁磊), Yi-Ting Xu(徐一汀), Guo-Chun Zhang(张国春), Zhi-Min Wang(王志敏), Yong Bo(薄勇), Qin-Jun Peng(彭钦军), Da-Fu Cui(崔大复), Yi-Cheng Wu(吴以成), Zu-Yan Xu(许祖彦)
Chin. Phys. B . 2018, 27(5): 054211. **doi:** 10.1088/1674-1056/27/5/054211

Responsive mechanism and molecular design of di-2-picolylamine-based two-photon fluorescent probes for zinc ions

Mei-Yu Zhu(朱美玉), Ke Zhao(赵珂), Jun Song(宋军), Chuan-Kui Wang(王传奎)
Chin. Phys. B . 2018, 27(2): 023302. **doi:** 10.1088/1674-1056/27/2/023302

Temperature dependence of line parameters of $^{12}C^{16}O_2$ near 2.004 μm studied by tunable diode laser spectroscopy

Hongliang Ma(马宏亮), Mingguo Sun(孙明国), Shenlong Zha(查申龙), Qiang Liu(刘强), Zhensong Cao(曹振松), Yinbo Huang(黄印博), Zhu Zhu(朱柱), Ruizhong Rao(饶瑞中)
Chin. Phys. B . 2018, 27(2): 023301. **doi:** 10.1088/1674-1056/27/2/023301

Responsive mechanism of 2-(2'-hydroxyphenyl)benzoxazole-based two-photon fluorescent probes for zinc and hydroxide ions

Zhang Yu-Jin, Zhang Qiu-Yue, Ding Hong-Juan, Song Xiu-Neng, Wang Chuan-Kui
Chin. Phys. B . 2015, 24(2): 023301. **doi:** 10.1088/1674-1056/24/2/023301

Isomerism and coordination mode effects on two-photon absorption of tris(picolyl)amine-based fluorescent probes for zinc ions*

Ke Zhao(赵珂)†, Jun Song(宋军), Mei-Yu Zhu(朱美玉), Han Zhang(张瀚), and Chuan-Kui Wang(王传奎)

School of Physics and Electronics, Shandong Normal University, Jinan 250358, *China*

(Received 8 March 2018; revised manuscript received 25 July 2018; published online 10 September 2018)

One-photon absorption and two-photon absorption (TPA) properties of three tris(picolyl)amine-based zinc ion sensors are investigated by employing the density functional response theory in combination with the polarizable continuum model. The different isomer and coordination geometry of each probe are taken into account. Special emphasis is placed on the effects of isomerism and the coordination mode on the optical properties. The intra-molecular charge transfer (ICT) properties are specified by natural bond orbital charge analysis. It is shown that the isomerism has non-negligible effects on TPA properties of free ligands. It is found that both the TPA wavelength and the cross section are highly dependent on the coordination mode. When the zinc ion connects with the picolyl unit in the middle of a ligand, the zinc complex has a large TPA intensity in a long wavelength range due to the increased ICT mechanism.

Keywords: two-photon absorption, isomerism, coordination mode, zinc ion

PACS: 33.20.–t, 42.65.–k, 82.30.Fi **DOI:** 10.1088/1674-1056/27/10/103301

1. Introduction

Great progress has been made in the imaging of living cells and tissues since the first two-photon fluorescence microscopy (TPM) appeared in 1990.[1] Compared with one-photon microscopy, TPM, in which two near-infrared photons for excitation are used, offers several advantages, including increased penetration depth, lower tissue auto-fluorescence and self-absorption, as well as reduced photo-damage and photo-bleaching.[2–4] As such, to facilitate the utility of TPM in bioimaging applications, there is a strong need to design two-photon (TP) probes for specific applications. To date, a variety of TP probes for diverse analytes, such as cation and anion ions,[5–8] pH values,[9,10] small molecules,[11,12] and DNA,[13] have been developed and their performances in bioimaging applications have been explored.

Zinc ion is the second most abundant transition metal ion in the living body. It plays an important role in many biological processes.[14–16] The dysbolism of zinc ions will result in many human diseases such as dysimmunity, Alzheimer's, and Parkinson's diseases. Therefore, it is necessary to detect the spatiotemporal distributions of the zinc ions in living systems. Recently, a number of zinc ion TP probes have been synthesized and their bioimaging applications have been demonstrated.[5,6] However, the related theoretical study is still very limited.[17–21] Wang *et al.*[17] designed a series of TP probes for zinc ions based on the intra-molecular charge transfer (ICT) mechanism. The one-photon absorption (OPA), two-photon absorption (TPA), and fluorescence properties were calculated. It was found that the designed probes can become fluorescent bioimaging reagents used for ratiometric detection. Bednarska *et al.*[18] investigated the responsive mechanism for a bipyridine-centered ratiometric zinc ions probe theoretically. The electric structure and nonlinear absorption spectra were calculated including solute-solvent interactions. Their results indicated that nonlinear response functions combined with density functional theory (DFT) can be successful in analyzing metal ion probes. In our previous researches,[19–21] response theory was used to investigate the OPA and TPA of a series of zinc ion sensors. The responsive mechanisms were specified at length, and a series of TP probes was designed by taking the established structure-property relationships into account.

In this paper, we choose three zinc ion TP probes 1, 2, and 3 (see Fig. 1) as the model molecules. It was reported that probe 1 undergoes a significant increase of the TPA cross sections by the Zn^{2+}-coordination induced ICT enhancement.[22] To explore the recognition mechanisms of the probes and the structure-property relationships, we perform a theoretical study on the OPA and TPA properties of the probes before and after combination with Zn^{2+} using DFT. In our study, it is interesting to find that these probes could have several isomeric geometries and then the corresponding zinc complexes pose various coordination modes. Therefore, we put an emphasis on the effects of isomerism and coordination mode on the TPA properties for the probe isomers and their zinc complexes.

Although isomerism is quite a common phenomenon

*Project supported by the Natural Science Foundation of Shandong Province, China (Grant No. ZR2014AM026) and the Taishan Scholar Project of Shandong Province, China.

†Corresponding author. E-mail: zhaoke@sdnu.edu.cn

© 2018 Chinese Physical Society and IOP Publishing Ltd

in chemistry, the effects of isomerism on TPA properties of organic molecules have seldom been discussed in the literature.[23,24] In our previous researches,[25–29] we investigated the influences of isomerism on TPA properties for a series of TPA active molecules. For a probe in solution at room temperature, various isomers of free and bound fluorophores are possible and produce specific spectral features. It is therefore highly required to take isomerism and coordination mode effects into account. To the best of our knowledge, these effects have not been investigated theoretically for TP metal ion sensors. Our research will provide a good understanding of the experimental observations for TP metal ion probes.

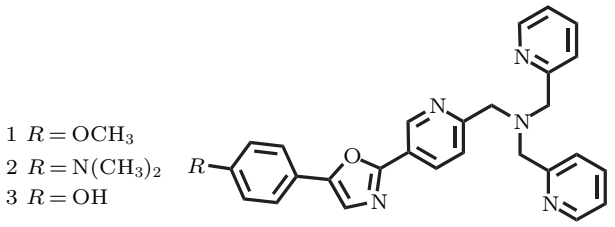


Fig. 1. Chemical structures of probes 1, 2, and 3.

2. Computational method

The oscillator strength can be used to describe the intensity of OPA. It is expressed as:

$$f_{\mathrm{op}} = \frac{2\omega_f}{3}\sum_{\alpha}|\langle 0|\mu_\alpha|f\rangle|^2, \tag{1}$$

where $\alpha \in (x,y,z)$, μ_α is the dipole moment operator, and ω_f denotes the excitation energy from the ground state $\langle 0|$ to the excited state $|f\rangle$.

In the case of resonant degenerate TPA, the sum-over-state expression for the two-photon matrix element can be written as[30]

$$S_{\alpha\beta} = \sum_s \left(\frac{\langle 0|\,\mu_\alpha\,|s\rangle\,\langle s|\,\mu_\beta\,|f\rangle}{\omega_s - \omega} + \frac{\langle 0|\,\mu_\beta\,|s\rangle\,\langle s|\,\mu_\alpha\,|f\rangle}{\omega_s - \omega} \right), \tag{2}$$

where $\alpha,\beta \in (x,y,z)$, and ω is the fundamental frequency of the laser beam, and we assume that it is equal to half the excitation energy of the final state, i.e., $2\omega = \omega_f$; ω_s represents the excitation energy for the intermediate state $|s\rangle$. The summation here includes all intermediate, initial, and final states. In response theory, the two-photon matrix element $S_{\alpha\beta}$ can be calculated through the single residues of the quadratic response function.[31]

The microscopic TPA cross section of molecules excited by a linear polarized single beam can be expressed as[30,32]

$$\delta = \sum_{\alpha,\beta}(2S_{\alpha\alpha}S^*_{\beta\beta} + 4S_{\alpha\beta}S^*_{\alpha\beta}). \tag{3}$$

The macroscopic TPA cross section that can be directly compared with the experimental measurement, is defined as[32]

$$\sigma = \frac{4\pi^2 a_0^5 \alpha\omega^2}{15c\Gamma}\delta. \tag{4}$$

Here a_0 is the Bohr radius, c is the speed of light, and α is the fine structure constant. The level broadening Γ of the final state is assumed to have the commonly used value $\Gamma = 0.1$ eV. The TPA cross section is in units of GM, 1 GM = 10^{-50} cm^4·s/photon.

In this work, the geometries of molecules are fully optimized by using DFT with the 6-31G(d,p) basis set and the B3LYP hybrid functional. On the basis of the optimized structures, the OPA properties are computed by the time-dependent DFT (TD-DFT) approach at the B3LYP level with the 6-31G(d) basis set. All the calculations of optimization and OPA properties are carried out in the Gaussian 09 program.[33] The TPA cross sections are obtained by the response theory using the B3LYP functional with 6-31G(d) basis set in the Dalton 2013 package.[34] In addition, the effect of water solvent is taken into account through the self-consistent reaction field theory based on the polarizable continuum model (PCM) in both Gaussian and Dalton calculations. Our previous work has shown that the B3LYP functional calculations can give reasonable TPA properties which are consistent with the trend of experimental observations.[19–21,25–29] The use of bigger basis sets could probably provide better numerical results, but we believe that the overall picture would not change.

3. Results and discussion

3.1. Geometry optimization

Probe 1 as depicted in Fig. 1 is composed of an electron-donating anisole substituent and an electron-deficient tris(picolyl)amine Zn^{2+} receptor linked through an oxazole bridge. The tris(picolyl)amine unit often acts as the Zn^{2+} receptor in the TP probe. The nitrogen atom could coordinate with the zinc ion by donating a lone electron pair into an empty metal orbital. In probe 2, we replace the anisole donor with the dimethylamino terminal because the dimethylamino group has stronger ability to donate and transport electrons. In probe 3, the hydroxy group with weaker donation ability is used. These push-pull structures can improve the ICT and induce a large TPA response. The geometry optimization of probe 1 gives as many as six equilibrium conformations 1a–1f as shown in Fig. 2. The frequency calculations for these geometries do not produce any imaginary frequencies. It can be seen that the six isomers differ by the orientations of two picolyl groups at the end of the ligands. The optimized geometries of zinc complexes are also presented in Fig. 2. Two Cl^- ions are incorporated explicitly in order to include counter ion effects and

give the charge-neutral complex.[19,22] It is interesting to find that different coordination geometries are obtained. In Zn1a structure, the zinc ion prefers to chelate with four nitrogen atoms of the tris(picolyl)amine receptor to complete the six-coordination geometry. The bond length between the nitrogen atom and zinc ion has a typical value of 2.1 Å–2.3 Å, which is similar to the general x-ray crystal structure.[35] The Zn1b and Zn1c have similar structures, in which the zinc ion connects with the three nitrogen atoms of the dipicolylamine group at the end of the ligands. The Zn1d also has a five-coordination geometry, but one of the connecting nitrogen atoms belongs to the picolyl unit in the middle of the ligand. In Zn1e and Zn1f, only two nitrogen atoms take part in the coordination. In Zn1f, the zinc ion does not connect with the picolyl unit in the middle of the ligand. By examining these complexes' structures, one can find that the zinc ions in Zn1b, Zn1c, and Zn1f are a little farther away from the oxazole cores than the zinc ions in the other structures. It is also noticed that each of all the backbones for these structures has good planarity.

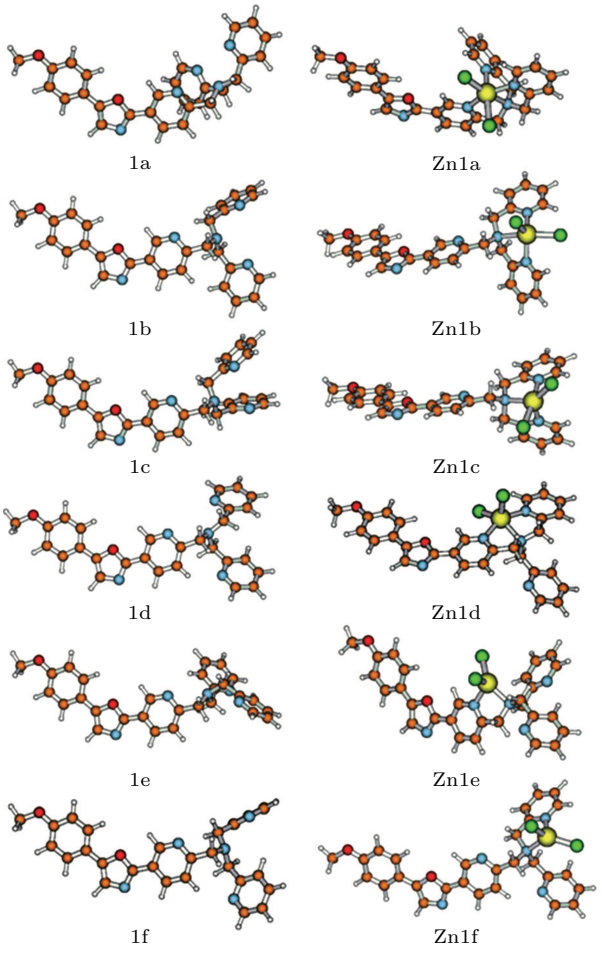


Fig. 2. (color online) Optimized geometries of 1a–1f and the corresponding zinc complexes.

The optimized geometries of probe 2 and the corresponding zinc complexes are displayed in Fig. 3. The result is the same as that of probe 1. Six isomers of probe 2 and six coordination conformations are also obtained. The corresponding geometries of probe 3 are also fully optimized.

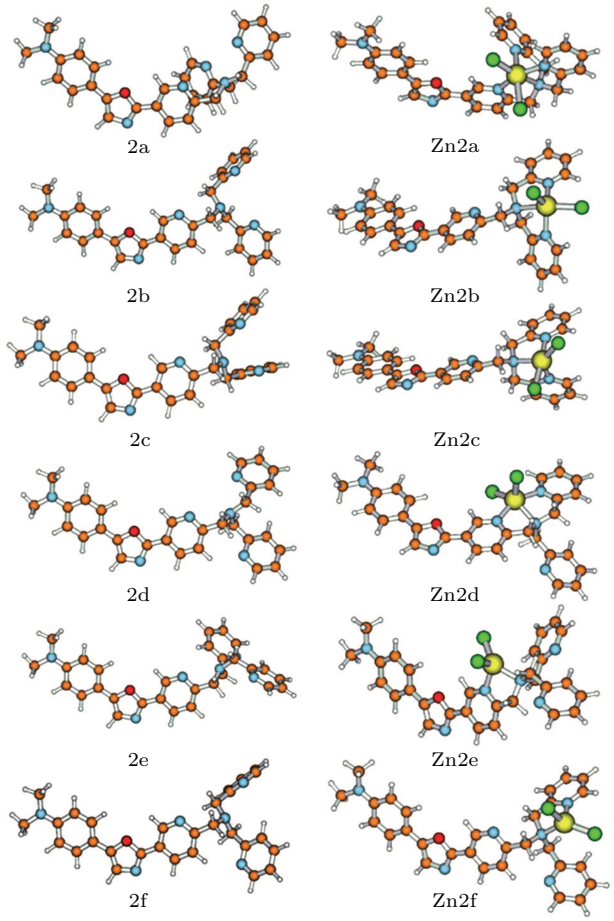


Fig. 3. (color online) Optimized geometries of 2a–2f and the corresponding zinc complexes.

It is expected that the various conformations will give rise to different electronic structures, which are closely related to the TPA transition matrix element according to Eq. (2). The permanent dipole moments and the energies of these structures are examined and the results are listed in Table 1. It shows that the permanent dipole moments of isomers 1a–1f are quite different: 1c has the largest dipole moment (7.584 deb, 1 deb = 3.33564×10^{-30} C · m), and 1d has the smallest one (3.037 deb). In the corresponding zinc complexes, the permanent dipole moments still maintain almost the same order. This result is consistent with the characteristics of the structures. It is found that 1f has the lowest energy among six isomers of probe 1, and the energy differences between the other structures and 1f are very small in general. The energy difference ΔE ranges from 1.8 kcal/mol to 4.1 kcal/mol. Such small energy barriers indicate that these isomers could be thermally populated. It is surprising that Zn1a has the lowest energy among the zinc complexes and the energy difference between Zn1e and Zn1a has the largest value, which is 11.04 kcal/mol. This is probably because Zn1a has a six-coordination geometry while Zn1e only has four coordination bonds. It is also found that the energy differences between Zn1a and Zn1b and between Zn1a and Zn1d are only

0.667 kcal/mol and 0.733 kcal/mol, which means that these structures can be populated at considerable percentages according to the Boltzmann distribution. The case of probe 2 is similar to that of probe 1. The difference in permanent dipole moment among the isomers becomes more obvious. However, for probe 3, the difference in permanent dipole moment among the isomers is a little smaller than for probe 1.

Table 1. Values of permanent dipole moment μ and energy difference ΔE.

	μ/D	ΔE/kcal·mol^{-1}		μ/D	ΔE/kcal·mol^{-1}
1a	4.276	4.050	Zn1a	17.955	0
1b	7.459	2.006	Zn1b	21.716	0.667
1c	7.584	3.603	Zn1c	23.215	9.074
1d	3.037	1.878	Zn1d	13.684	0.733
1e	4.403	0.062	Zn1e	14.841	11.040
1f	3.511	0	Zn1f	18.721	9.823
2a	3.631	4.056	Zn2a	16.623	0
2b	7.998	2.032	Zn2b	24.105	0.725
2c	9.355	3.603	Zn2c	26.522	9.134
2d	2.248	1.910	Zn2d	11.376	0.762
2e	6.281	0.092	Zn2e	12.611	10.749
2f	5.320	0	Zn2f	18.934	9.656
3a	4.423	4.046	Zn3a	18.150	0
3b	7.326	1.990	Zn3b	21.412	0.752
3c	7.138	3.578	Zn3c	22.553	9.039
3d	3.476	1.877	Zn3d	14.248	0.732
3e	4.085	0.043	Zn3e	15.684	10.864
3f	3.323	0	Zn3f	18.516	9.785

3.2. One-photon absorption

Our calculated OPA wavelength λ_{op}, oscillator strength f_{op}, and transition nature of all the studied molecules are listed in Table 2. It shows that the maximum OPA peaks of these compounds are all derived from the transition between ground state (S_0) and the first excited state (S_1), which is mainly dominated by the transition from the highest occupied molecular orbital (HOMO) to the lowest unoccupied molecular orbital (LUMO).

For probe 1, one can see that the OPA wavelengths of the six isomers 1a–1f are all located at about 360 nm and their oscillator strengths only have a little difference. When the molecule binds to a zinc ion, the λ_{op} is red-shifted or blue-shifted to some extent. The Zn1a, Zn1d, Zn1e, and Zn1f have 16-, 21-, 28-, and 7-nm red-shifts respectively, while Zn1b and Zn1c have 4- and 3-nm blue-shift. The largest red-shift occurs in Zn1e. As a result, various coordination conformations have different OPA wavelengths. It also shows that the differences in oscillator strength among these zinc complexes increase in comparison with those among free ligands. The f_{op} of Zn1e is 0.7, which is much lower than the value of Zn1f, 0.99. These results indicate that the coordination modes have some effects on OPA properties. One can conclude that when the zinc ion coordinates with the nitrogen atom, which belongs to the picolyl unit in the middle of the ligand, the OPA wavelength has a considerable red-shift.

From probe 1 to probe 2 it follows that the OPA wavelengths of 2a–2f are red-shifted to around 410 nm due to the stronger electron donor. The isomerism still has very little effect on the OPA properties of the free ligands. However, when it comes to the zinc complexes, the various coordination modes have quite different OPA properties. The OPA wavelengths of Zn2a, Zn2d, and Zn2e are red-shifted obviously with respect to their free ligands. The largest red-shift still occurs in Zn2e, arriving at 48 nm. In addition, the difference in λ_{op} between Zn2b and Zn2e becomes 47 nm.

Table 2. One-photon absorption wavelength properties of the molecules in water solvent.

	λ_{op}/nm	f_{op}	Transition nature		λ_{op}/nm	f_{op}	Transition nature
1a	361	0.89	S_0–S_1 H–L(99%)	Zn1a	377	0.71	S_0–S_1 H–L(96%)
1b	362	0.90	S_0–S_1 H–L(89%)	Zn1b	358	0.98	S_0–S_1 H–L(99%)
1c	364	0.85	S_0–S_1 H–L(86%)	Zn1c	361	0.93	S_0–S_1 H–L(99%)
1d	357	1.01	S_0–S_1 H–L(99%)	Zn1d	378	0.76	S_0–S_1 H–L(99%)
1e	359	0.98	S_0–S_1 H–L(99%)	Zn1e	387	0.70	S_0–S_1 H–L(99%)
1f	359	1.02	S_0–S_1 H–L(97%)	Zn1f	366	0.99	S_0–S_1 H–L(99%)
2a	411	0.73	S_0–S_1 H–L(99%)	Zn2a	438	0.57	S_0–S_1 H–L(99%)
2b	408	0.84	S_0–S_1 H–L(99%)	Zn2b	410	0.76	S_0–S_1 H–L(96%)
2c	408	0.83	S_0–S_1 H–L(99%)	Zn2c	414	0.74	S_0–S_1 H–L(96%)
2d	405	0.84	S_0–S_1 H–L(99%)	Zn2d	442	0.60	S_0–S_1 H–L(99%)
2e	409	0.81	S_0–S_1 H–L(99%)	Zn2e	457	0.54	S_0–S_1 H–L(99%)
2f	406	0.86	S_0–S_1 H–L(99%)	Zn2f	412	0.80	S_0–S_1 H–L(99%)
3a	358	0.84	S_0–S_1 H–L(98%)	Zn3a	374	0.67	S_0–S_1 H–L(99%)
3b	360	0.82	S_0–S_1 H–L(86%)	Zn3b	358	0.88	S_0–S_1 H–L(99%)
3c	363	0.72	S_0–S_1 H–L(79%)	Zn3c	355	0.93	S_0–S_1 H–L(99%)
3d	354	0.92	S_0–S_1 H–L(96%)	Zn3d	375	0.72	S_0–S_1 H–L(99%)
3e	357	0.93	S_0–S_1 H–L(98%)	Zn3e	385	0.65	S_0–S_1 H–L(99%)
3f	357	0.96	S_0–S_1 H–L(96%)	Zn3f	363	0.94	S_0–S_1 H–L(99%)

The OPA properties of probe 3 are similar to those of probe 1 due to the little difference in the donation ability between the methoxy and the hydroxy groups. Nearly all the OPA wavelengths of 3a–3f and Zn3a–Zn3f are slightly blue-shifted compared with those of the corresponding structures 1a–1f and Zn1a–Zn1f.

3.3. Two-photon absorption

The TPA wavelength λ_{tp} and cross section σ in water solvent for all the studied molecules are calculated by the response theory in the Dalton program. The TPA cross sections of the three lowest excited states for probes 1 and 2 are presented in Table 3.

Table 3. Values of two-photon absorption wavelengths λ_{tp} and cross section σ of the three lowest excited states of probes 1 and 2 in water solvent.

	State	λ_{tp}/nm	σ/GM		State	λ_{tp}/nm	σ/GM
1a	S_1	732	224	Zn1a	S_1	773	367
	S_2	678	7		S_2	668	1
	S_3	599	94		S_3	649	6
1b	S_1	740	97	Zn1b	S_1	736	279
	S_2	704	290		S_2	685	2
	S_3	609	43		S_3	670	1
1c	S_1	743	74	Zn1c	S_1	745	317
	S_2	703	373		S_2	691	3
	S_3	606	52		S_3	620	17
1d	S_1	727	237	Zn1d	S_1	778	403
	S_2	707	14		S_2	672	1
	S_3	606	9		S_3	647	13
1e	S_1	732	260	Zn1e	S_1	808	439
	S_2	689	12		S_2	709	16
	S_3	597	91		S_3	586	37
1f	S_1	736	195	Zn1f	S_1	752	375
	S_2	674	233		S_2	713	1
	S_3	597	69		S_3	612	69
2a	S_1	822	538	Zn2a	S_1	893	658
	S_2	667	11		S_2	761	14
	S_3	659	45		S_3	730	16
2b	S_1	824	538	Zn2b	S_1	838	596
	S_2	693	240		S_2	790	16
	S_3	661	29		S_3	770	1
2c	S_1	824	524	Zn2c	S_1	850	627
	S_2	703	285		S_2	800	19
	S_3	659	30		S_3	705	2
2d	S_1	816	570	Zn2d	S_1	906	716
	S_2	695	3		S_2	766	14
	S_3	646	93		S_3	754	13
2e	S_1	824	586	Zn2e	S_1	951	723
	S_2	678	10		S_2	819	66
	S_3	658	37		S_3	670	31
2f	S_1	824	567	Zn2f	S_1	865	761
	S_2	668	252		S_2	841	1
	S_3	656	27		S_3	695	43

For 1a, 1d, and 1e, the first excited state has the largest TPA intensity. The largest cross sections of 1a, 1d, and 1e are located at about 730 nm with 224, 237, and 260 GM respectively. As for 1b and 1c, the second excited state has the largest TPA intensity and the corresponding TPA wavelength λ_{tp} is centered at around 700 nm. The values of σ are equal to 290 GM and 373 GM. For 1f, both the first and the second excited states have considerable TPA cross sections. We note that the isomerism effects cannot be neglected. If all the isomers are taken into account, the obtained TPA spectrum could have several separated absorption maxima at about 670 nm, 700 nm, and 730 nm respectively.

When coordinated with Zn^{2+}, the first excited state has the largest TPA intensity for all the zinc complexes. One can see that the coordination mode has an important effect on the TPA property. There are big differences in not only TPA intensity but also wavelength among zinc complexes. The largest cross section of Zn1a is 367 GM at 773 nm. The TPA wavelengths of Zn1b and Zn1c are 736 nm and 745 nm respectively, which are much shorter than that of Zn1a. Zn1b has the smallest cross section, which is only 279 GM. The λ_{tp} of Zn1d is similar to that of Zn1a, but the σ increases to 403 GM. Zn1e has the longest λ_{tp}, 808 nm, and the largest σ, 439 GM. That is, the absorption position ranges from 736 nm to 808 nm, which means that the absorption bands have large shifts between each other. From the cross section, we find that the TPA intensity is in the order Zn1e>Zn1d>Zn1f>Zn1a>Zn1c>Zn1b. The difference between the maximum and the minimum cross sections is large, which is 160 GM, about 36% of the maximum. By the inspection of the structures of the zinc complexes, one can quickly realize that the coordination mode with the connection between the zinc ion and the nitrogen atoms, which belongs to the picolyl unit in the middle of the ligand, always brings about the large cross sections in a long wavelength region. According to Eq. (2), we know that the TPA transition matrix element is determined by the electronic structures including the dipole moments and the excitation energies. So the lowest excitation energy of Zn1e is one of the probable reasons for the strongest TPA intensity among the zinc complexes. Comparing with corresponding free ligands, λ_{tp} has a large red-shift and σ is increased greatly for Zn1a, Zn1d, and Zn1e. These results are in good agreement with experimental observations.[22] The arrangement where the metal ion binds to the acceptor site should yield an increased cross section.[19,22]

In the case of probe 2, the first excited state has the largest TPA intensity for all the free ligands and zinc complexes. For 2b, 2c, and 2f, the second excited state also has considerable intensity. The largest cross sections of 2a–2f are all located at about 820 nm with different cross sections. The maximum and the minimum cross sections are 524 GM and 586 GM for 2c and 2e respectively. Both 2b and 2c have two absorption maxima at about 820 nm and 700 nm and the absorption intensities at 700 nm cannot be neglected. As for probe 1, if all the isomers 2a–2f are considered together, the obtained TPA spectrum could have several separated absorption maxima. One

can also see that the TPA wavelengths have large red-shifts and the intensities increase greatly due to the stronger electron donor with respect to probe 1.

Table 4. Value of two-photon absorption wavelength λ_{tp} and cross section σ of three lowest excited states of probe 3 in water solvent.

	State	λ_{tp}/nm	σ/GM		State	λ_{tp}/nm	σ/GM
3a	S_1	730	207	Zn3a	S_1	775	345
	S_2	681	8		S_2	670	1
	S_3	597	84		S_3	646	5
3b	S_1	738	86	Zn3b	S_1	745	297
	S_2	701	281		S_2	689	6
	S_3	609	37		S_3	672	1
3c	S_1	743	46	Zn3c	S_1	738	271
	S_2	703	391		S_2	697	1
	S_3	609	29		S_3	621	1
3d	S_1	725	218	Zn3d	S_1	783	386
	S_2	707	16		S_2	676	1
	S_3	608	8		S_3	653	13
3e	S_1	732	244	Zn3e	S_1	816	414
	S_2	685	8		S_2	715	22
	S_3	596	75		S_3	586	31
3f	S_1	732	153	Zn3f	S_1	754	360
	S_2	674	226		S_2	717	1
	S_3	595	58		S_3	615	57

Upon Zn^{2+} binding, each of all the zinc complexes has a strong TPA peak in a longer wavelength range with enhanced cross section in comparison with each of the corresponding free ligands. It shows that the TPA wavelength and cross section are quite different among the zinc complexes. Zn2b has the smallest cross section 596 GM at 838 nm, while Zn2f has the largest value 761 GM at 865 nm. The cross section increases by 165 GM. Like the zinc complexes of probe 1, the TPA intensity is in the order Zn2f>Zn2e>Zn2d>Zn2a>Zn2c>Zn2b. When the zinc ion connects with the nitrogen atoms from the picolyl unit in the middle of the ligand, Zn2e, Zn2d, and Zn2a give rise to the large cross sections in the long wavelength region. Although Zn2f has the largest cross section, the TPA wavelength is located at 865 nm, which is much shorter than those of Zn2e, Zn2d, and Zn2a. According to our calculations, it can be concluded that the coordination mode plays an important role in TPA intensity and wavelength.

The TPA properties of probe 3 are also calculated and the results are shown in Table 4. The data are similar to those of probe 1. Most of the TPA cross sections decrease a little with respect to the corresponding structures of probe 1 due to the weak donor unit.

3.4. Intra-molecular charge transfer

It is well known that TPA properties highly depend on the ICT process. The charge will be redistributed when the molecule is excited from the ground state to the excited state. In order to further explore the effects of the coordination mode and obtain a better understanding of the ICT process, we perform the natural bond orbital charge analyses for Zn1a, Zn1b, Zn1d, and Zn1e in their ground states and in the first excited states. To analyze them clearly, these molecules are divided into three parts as shown in Fig. 4. The net charges of parts A, B, and C are specifically calculated and all the calculated results are listed in Table 5.

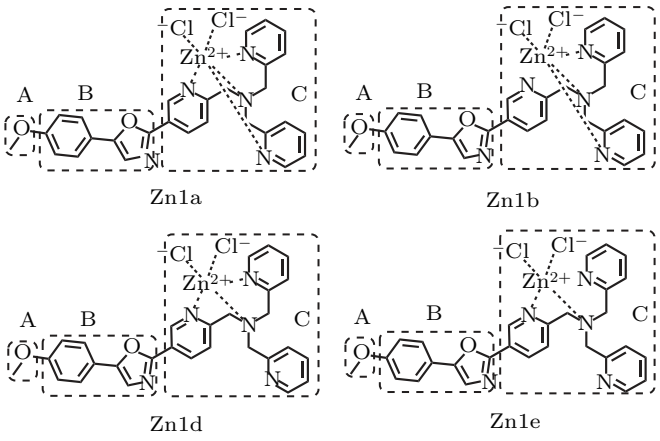


Fig. 4. Divided parts of the molecules Zn1a, Zn1b, Zn1d, and Zn1e.

Table 5. Net charges (in units of e) for divided parts of the molecules in the ground states and in the first excited states.

	Q_{A0}	Q_{A1}	ΔQ_A	Q_{B0}	Q_{B1}	ΔQ_B	Q_{C0}	Q_{C1}	ΔQ_C
Zn1a	–0.186	–0.102	0.084	0.224	0.544	0.320	–0.037	-0.441	-0.404
Zn1b	–0.187	–0.114	0.073	0.204	0.430	0.226	–0.017	-0.316	-0.299
Zn1d	–0.186	-0.101	0.085	0.226	0.550	0.324	–0.041	–0.450	-0.409
Zn1e	–0.185	–0.096	0.089	0.236	0.586	0.350	–0.051	–0.490	-0.439

Q_{A0} and Q_{A1} denote the net charge of part A in the ground state and that in the first excited state, respectively. ΔQ_A represents the net charge difference between the ground state and the first excited state in part A. Like this definition, ΔQ_B and ΔQ_C denote the net charge differences between the ground state and the first excited state for part B and part C, respectively. For Zn1a, it is found that the net charge of part A in the first excited state Q_{A1} is $-0.102e$, which is more electropositive than the value in the ground state Q_{A0}, $-0.186e$. The net charge of part B in the first excited state (Q_{B1}, $0.544e$) is also more electropositive than in the ground state (Q_{B0}, $0.224e$). In the case of part C, the net charge in the first excited state

(Q_{C1}, $-0.441e$) is more electronegative than in the ground state (Q_{C0}, $-0.037e$). This indicates that part A, together with part B, is the donor, and part C is the acceptor of the molecule. Other structures are similar to those of Zn1a. That is, part A and part B both act as a donor, and part C serves as an acceptor. The net charge difference of the donor should be the sum of ΔQ_A and ΔQ_B. For Zn1a, the net charge difference of the donor is $0.404e$, which is very close to the value of Zn1d, $0.409e$. Zn1b has the smallest value, $0.299e$ and Zn1e has the biggest one, $0.439e$. This demonstrates that the capacity of ICT is in the order Zn1e>Zn1d>Zn1a>Zn1b, which is consistent with the order of TPA intensity.

4. Conclusions

Effects of isomerism and coordination mode on the linear and nonlinear optical properties of three TP probes for zinc ions are theoretically studied by quantum chemical calculations. Six isomers and six corresponding zinc complexes of each probe are optimized and their OPA and TPA properties are calculated at the DFT level. Also, the ICT properties for various coordination conformations are specified. It is found that the isomerism has some effects on TPA properties of free ligands and cannot be neglected. The TPA wavelength and cross section are quite different among the zinc complexes, which demonstrates the significant coordination mode effects on TPA. It is interesting to find the coordination modes where the zinc ion connects with the picolyl unit in the middle of the ligand always give rise to the large cross sections in a long wavelength region. The natural bond orbital charge analysis shows that this coordination conformation has the strongest ICT capacity. Our results provide useful information for understanding the TPA properties of metal ion probes.

References

[1] Denk W, Strickler J H and Webb W W 1990 *Science* **248** 73
[2] Yao S and Belfield K D 2012 *Eur. J. Org. Chem.* **2012** 3199
[3] Kim D, Ryu H G and Ahn K H 2014 *Org. Biomol. Chem.* **12** 4550
[4] Kim H M and Cho B R 2015 *Chem. Rev.* **115** 5014
[5] Kim H M and Cho B R 2011 *Chem. Asian J.* **6** 58
[6] Sarkar A R, Kang D E, Kim H M and Cho B R 2014 *Inorg. Chem.* **53** 1794
[7] Sumalekshmy S and Fahrni C J 2011 *Chem. Mater.* **23** 483
[8] Kim D, Singha S, Wang T, Seo E, Lee J H, Lee S J, Kim K H and Ahn K H 2012 *Chem. Commun.* **48** 10243
[9] Kim H M, An M J, Hong J H, Jeong B H, Kwon O, Hyon J Y, Hong S C, Lee K J and Cho B R 2008 *Angew. Chem. Int. Ed.* **47** 2231
[10] Kim H J, Heo C H and Kim H M 2013 *J. Am. Chem. Soc.* **135** 17969
[11] Das S K, Lim C S, Yang S Y, Han J H and Cho B R 2012 *Chem. Commun.* **48** 8395
[12] Masanta G, Heo C H, Lim C S, Bae S K, Cho B R and Kim H M 2012 *Chem. Commun.* **48** 3518
[13] Zhang Y, Wang J, Jia P, Yu X, Liu H, Liu X, Zhao N and Huang B 2010 *Org. Biomol. Chem.* **8** 4582
[14] Bush A I, Pettingell W H, Multhaup G, Paradis M D, Vonsattel J P, Gusella J F, Beyreuther K, Masters C L and Tanzi R E 1994 *Science* **265** 1464
[15] Cuajungco M P and Lees G J 1997 *Neurobiol. Dis.* **4** 137
[16] Bush A I and Tanzi R E 2002 *Proc. Natl. Acad. Sci. USA* **99** 7317
[17] Wang D, Guo J F, Ren A M, Huang S, Zhang L and Feng J K 2014 *J. Phys. Chem. B* **118** 10101
[18] Bednarska J, Zaleśny R, Murugan N A, Bartkowiak W, Ågren H and Odelius M 2016 *J. Phys. Chem. B* **120** 9067
[19] Zhu M Y, Zhao K, Song J and Wang C K 2018 *Chin. Phys. B* **27** 023302
[20] Zhang Y J, Zhang Q Y, Ding H J, Song X N and Wang C K 2015 *Chin. Phys. B* **24** 023301
[21] Zhu M Y, Song J and Zhao K 2017 *J. At. Mol. Sci.* **8** 152
[22] Sumalekshmy S, Henary M M, Siegel N, Lawson P V, Wu Y, Schmidt K, Brédas J L, Perry J W and Fahrni C J 2007 *J. Am. Chem. Soc.* **129** 11888
[23] Arnbjerg J, Jiménez-Banzo A, Paterson M J, Nonell S, Borrell J I, Christiansen O and Ogilby P R 2007 *J. Am. Chem. Soc.* **129** 5188
[24] Guillaume M, Ruud K, Rizzo A, Monti S, Lin Z and Xu X 2010 *J. Phys. Chem. B* **114** 6500
[25] Zhao K, Liu P W, Wang C K and Luo Y 2010 *J. Phys. Chem. B* **114** 10814
[26] Wang F Q, Zhao K, Zhu M Y and Wang C K 2016 *J. Phys. Chem. B* **120** 9708
[27] Jia H H, Zhao K and Wu X L 2014 *Chem. Phys. Lett.* **612** 151
[28] Zhao K, Han G C, Zhang L L and Jia H H 2014 *Chin. J. Chem. Phys.* **27** 75
[29] Wu X L, Zhao K, Jia H H and Wang F Q 2015 *Acta Phys. Sin.* **64** 233301 (in Chinese)
[30] Luo Y, Norman P, Macak P and Ågren H 2000 *J. Phys. Chem. A* **104** 4718
[31] Olsen J and Jørgensen P 1985 *J. Chem. Phys.* **82** 3235
[32] Monson P R and McClain W M 1970 *J. Chem. Phys.* **53** 29
[33] GAUSSIAN 09 References in http://www.gaussian.com/
[34] DALTON 2013 A molecular electronic structure program, Release Dalton2013.0 see http://daltonprogram.org/
[35] Xue L, Fang Z, Li G, Wang H and Jiang H 2011 *Sens. Actuator B-Chem.* **156** 410